IRANIAN JOURNAL OF CATALYSIS

# Sonochemical synthesis of undoped and Co-doped ZnO nanostructures and investigation of optical and photocatalytic properties

Bahar Khodadadi*, Maryam Bordbar

*Department of Chemistry, Faculty of Science, University of Qom, Qom, Iran.*

Received 25 January 2014; received in revised form 18 April 2015; accepted 10 June 2015

ABSTRACT

In this paper, undoped ZnO and Co-ZnO nano structures with different molar ratio of Cobalt have been synthesized by the sonochemical method. Structure have been characterized by Fourier Transform (FTIR) and UV–Vis spectroscopy, field emission Scanning Electron Microscopy (FE-SEM), Energy Dispersive Analytical X-Ray (EDAX), and X-Ray Diffraction (XRD) methods. Moreover, the direct band gap has been calculated by Tauc's approach. Moreover, mean crystal size has been estimated by Scherrer equation. Furthermore, photocatalytic activity for all samples has been investigated under UV irradiation in an aqueous medium. Compared with pure ZnO, the band gap of the Co-ZnO has been shown decrease and it is dependent on the content of dopants. Also, photocatalytic activity improves in the presence of cobalt dopant.

***Keywords***: *Sonochemical method, Band gap, Photocatalytic activity, ZnO nanostructure.*

## 1. Introduction

ZnO nanostructures have attracted a great deal of attention due to their unique properties such as: piezoelectric, semiconducting and catalytic activity and wide range of applications in sensors, solar cells, optoelectronics, and transducers in medical sciences. Also owing to high photocatalytic activity, low cost and environmentally friendly feature, ZnO has been widely used as a photocatalyst [1].

However, due to a wide band gap of 3.37 eV, poor photon absorption of ZnO limits its application as photocatalyst [2]. In order to improve the efficiency of photocatalytic activity various techniques such as increase of surface area using the production of nano dimension, control of the design shape, incorporating another atom into the lattice and so on can be used.

The presence of metals on ZnO which act as electron–hole separation centers can enhance the degradation efficiency of photocatalytic reactions [3,4]. Metal doped ZnO particles have attracted investigations because it is very easy to apply in many methods for preparing ZnO materials and properties of ZnO highly depend on dopant and nanostructures [5,6].

*Corresponding author email: khodadadi@qom.ac.ir
Tel: +98 25 3210 3792; Fax: +98 25 3285 0953

The control of properties for metal-doped ZnO and band gap engineering of nanomaterials is of utmost importance for tunable light emitting diodes (LEDs) and other optoelectronic devices. $Co^{2+}$ has close ionic radius parameter to that of $Zn^{2+}$, which means that this element can easily penetrate into ZnO crystal lattice or substitute $Zn^{2+}$ position in crystal [7].

Varieties of methods including sol–gel, precipitation, micro-emulsion, solvo-thermal, hydrothermal have been employed to synthesis ZnO nanomaterial. But, the sonochemical method has been proved to be a useful method to obtain novel materials [8–10]. Although, this technique provides a very quick, simple, and cost-effective route to nanostructures under ambient conditions [11]. Ultrasonic irradiation generates small bubbles in liquid medium and there is repeated formation, growth, and collapse of these bubbles in liquid medium this phenomenon is known as acoustic cavitation. An implosive collapse of cavitation bubbles by adiabatic compression results in very high temperature of 5000 K and high pressure [12, 13].

In this study, we have synthesized ZnO nanostructure and ZnO doped with Co, by sonochemical method with different molar ratio of Co in order to investigation of Co-doped effect on band gap and photocatalytic activity. Also, starch as important natural organic

compounds abundant in nature has used for controlling morphology of nanostructure.

## 2. Experimental

### *2.1. Materials and instruments*

Zinc acetate (Zn $(CH_3COO)_2$), absolute ethanol, double distilled water, Cobalt Nitrate $(Co(NO_3)_2.5H_2O)$, ethanol, sodium hydroxide (NaOH), starch, and acetone (for drying).

These materials were used without any further purification and were purchased from Merck Chemical Company.

The UV–Vis absorption spectra were measured under the diffuse reflectance mode in the range of 205–1000 nm with a PerkinElmer Lambda 25 UV–Vis spectrophotometer. Fourier transform infrared spectroscopy (FT-IR) analysis was carried out on a Varian model 640 spectrophotometer to determine the specific functional groups present on the surface and impurities of synthesized samples. XRD measurements were performed using a Philips x' pert pero MPD diffractometer with $CuK_\alpha$ radiation from 10 to 90 (2θ) at room temperature.

### *2.2. Sample preparation*

All samples were prepared by sonochemical method using the following procedure.

#### *2.2.1. Preparation of sample 1: (ZnO nanostructure)*

**A:** 0.025 g starch was dissolved in 10 ml of double distilled water and stirred until complete dissolution was achieved.

**B:** 10 ml of 0.1 M aqueous solution of zinc acetate and 10 ml 1 M aqueous solution of sodium hydroxide were added to 25 ml alcohol.

**C:** Solution **B** was added into solution **A** and then was immediately kept in sonication bath (33 KHz, 350 W) at room temperature for 4 h. Initial temperature of reaction mixture was 27°C. However, after 4 h temperature had risen to 57 °C. The white precipitate formed was collected by centrifugation and then thoroughly washed with water followed by ethanol to remove traces of starch and other impurities and then kept in vacuum oven for drying [1].

#### *2.2.2. Preparation of sample 2 (ZnO-Co (0.5%)) and sample 3 (Co-ZnO (1.0%))*

In this set of experiment, samples were prepared exactly such as sample 1 but two concentration of $Co(NO_3)_2$ (with molar ratio [Co]/ZnO=0.005, 0.01) was added to solution **B**. The other steps were repeated such as sample 1.

### *2.3. Photocatalysis conditions*

Methylene blue (MB) has often been used as a model dye molecule for photocatalytic degradation examination of samples. The photocatalytic activity of pure ZnO and Co- doped ZnO samples was evaluated by examining photocatalytic decomposition of MB dye under the irradiation of UV lights. These nanostructures could be utilized in numerous applications, especially for photo-degradation of organic pollutants [14]. All experiments were carried out in a photoreactor system with a capacity of 1 liter (Fig. 1).

MB (with a concentration of 5 $mgL^{-1}$) in deionized water was selected as pollutant solutions for photodegradation. These solutions were set in the vicinity of a nano photocatalyst powder (0.2 g powder in 1L solution) and were let in dark for 24 h to eliminate the absorptive effect of the solution in the catalyst. Then, it was placed in the photoreactor and methylene blue concentration change was recorded by UV spectroscopy. The photoreactor system which is shown in Fig. 1 consisted of a cubic borosilicate glass reactor with an effective volume of 1000 mL, a cooling water jacket and a 15 W UV lamp (Osram) with a quartz cover positioned inside the solution used as a UV light source. The reaction temperature was kept at 25 °C using cooling water.

## 3. Results and Discussion

### *3.1. FT-IR spectroscopy analysis*

Fig. 2 shows the FTIR spectra at room temperature in the range of 400–4000 $cm^{-1}$ of starch and ZnO nanostructures synthesized by sonochemical method. In undoped and doped ZnO samples, FTIR spectra were shown absorption band at ~3400 $cm^{-1}$ corresponds to the O–H stretching vibrations of starch or water presents in ZnO [1].

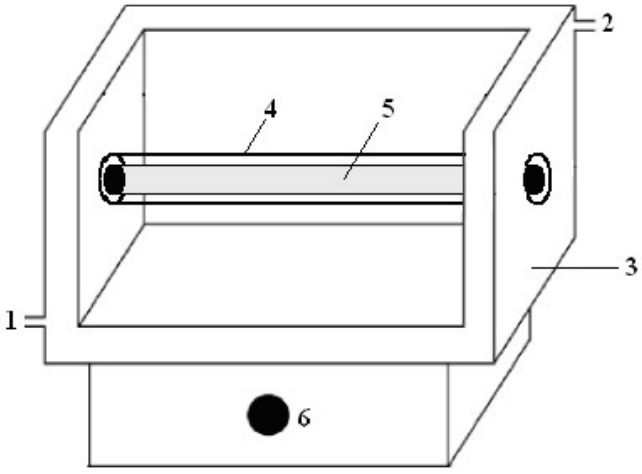


**Fig. 1.** Schematic diagram of the photoreactor system: 1- Water entrance, 2- Water exit, 3- Glass jacket, 4- Quartz cover, 5-UV lamp and 6-Stirrer.

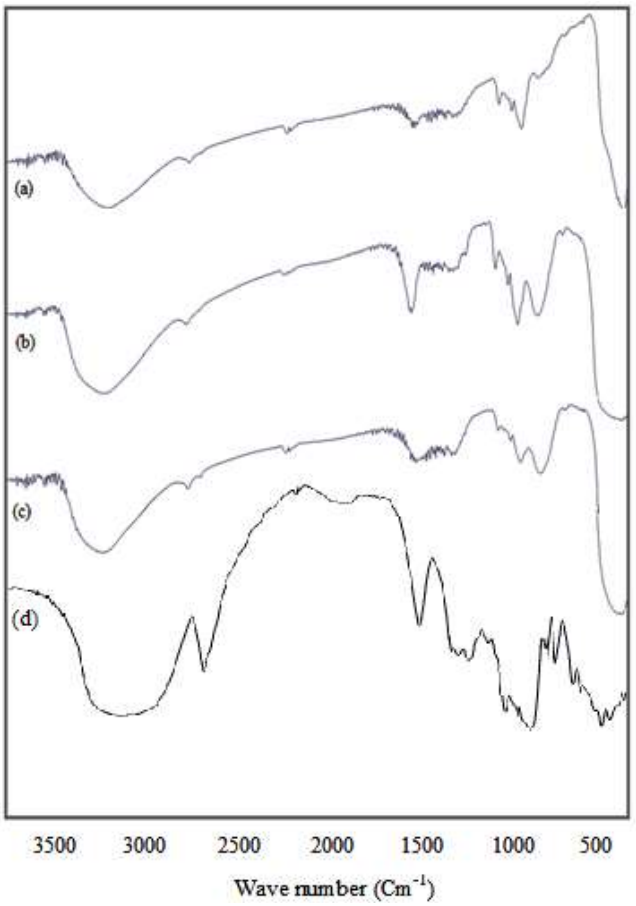


**Fig. 2.** FT-IR spectra of (a) undoped ZnO, (b) Co- ZnO (0.5%), (c) Co-ZnO (1%) and (d) starch.

In comparison with FTIR spectra of starch, the peaks at 900–1250 $cm^{-1}$ can be associated with the C–H stretching which shows that starch is present at surface of ZnO nano structure [1]. The band at ~1630 $cm^{-1}$ in samples, is related to the bending vibrations of adsorbed $H_2O$ molecules. In samples 2, and 3 which containing Cobalt as dopant, small peaks originated at around 890 $cm^{-1}$ is probably due to the Nitrate ($NO^{3-}$) groups [15,16].

Moreover, absorption band appearing between 400 $cm^{-1}$ and 600 $cm^{-1}$ corresponds to the stretching and vibrational modes of metal–oxygen (Co–O). Also, the stretching mode of ZnO nanostructure appears at 546 $cm^{-1}$ [17].

According to FT-IR spectra, no other distinguished peak is detected which related that metal atoms were successfully incorporated into the lattice of ZnO and the products have no significant impurity.

### *3.2. UV–visible spectroscopy and band gap calculation*

UV–Vis spectroscopy was performed to investigation of the optical properties of synthesized samples and results are reported in Fig. 3(a). The obtained UV– Vis spectrum for pure ZnO shows a single absorption band with the wavelengths of maximum absorbance at 354 nm that is characteristic band for the wurtzite hexagonal structure of ZnO [18]. According to these results, due to the doping of Cobalt into ZnO lattices the red shift in wavelengths of maximum absorbance are shown and maximum absorbance shifts slightly toward higher wavelength.

The absorption coefficients of samples were investigated by Tauc's approach [19], and the direct band gap is calculated using the following equation:

$$(\alpha h\nu)^2 = C\,(h\nu - E_g)$$

Where **α** is the absorption coefficient, C is a constant, h$\nu$ is the photon energy and $E_g$ is the band gap. Fig. 3(b), shows the Tauc plots of samples. Extrapolation of the linear region of Tauc plot gives a band gap. Table 1 show that increasing of dopant, reduced band gap and it is dependent on the content of dopants. Band gap value of 2.82 eV is obtained for pure ZnO nanostructure while the band gap of sample 2, and 3 were found to decrease upon increasing molar ratio of dopant and these results are consistent with UV-Vis spectra.

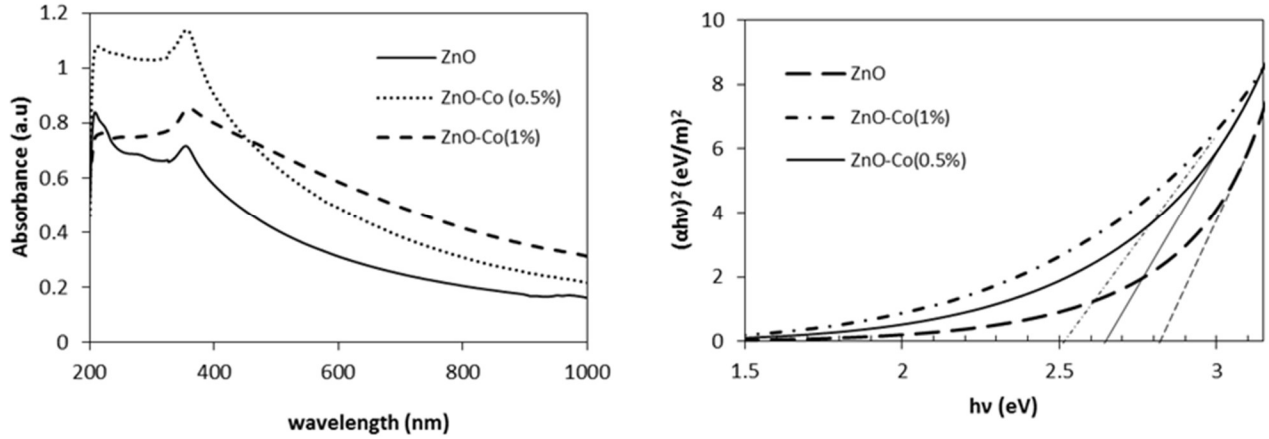


**Fig. 3**. (a) UV-Vis spectrum of undoped and Co-doped ZnO, (b) The Tauc plots of samples.

It seems that, formation of ZnO-Co bonds between Cobalt dopant and ZnO was the main reason for band gap decrease. In other words, the band gap ($E_g$) of pure ZnO can be tuned over a large energy range after Cobalt doping. The variation of the red-shifts of band gap after increase of Cobalt can be explain that, when Cobalt ions substituted Zn ion sites in the ZnO lattice, the band gap narrowed due to sp–d exchange interactions between the conduction band electrons and the d electrons of Cobalt ions. It can be said that, existence of Cobalt ions impurities in the ZnO structure, induce the formation of new recombination centers with lower emission energy and cause the narrowing band gap energy. Furthermore, the narrowing band gap energy after increasing the concentration of dopant ions is possibly due to development of a resonance structure in the density of states [20,21].

*3.3. XRD analysis*

The representative XRD patterns of the as-obtained samples are illustrated in Fig. 4. The diffraction patterns of samples are well in agreement with hexagonal wurtzite ZnO structure (JCPDS 01-080-0075) [22-24]. These results reveal that, no peaks corresponding to CoO or other Co-containing phases were detected in its XRD patterns, which demonstrates that Co ions have been entered into the lattices of ZnO substituting of $Zn^{2+}$ [25,26].

The lattice parameters of ZnO and Co–ZnO with different concentrations were calculated from the XRD by using the following equation [27]:

$$\frac{1}{d^2}=\frac{4}{3}\left(\frac{h^2+kh+k^2}{a^2}\right)+\frac{l^2}{c^2}$$

Where h, k and l are Miller indexes and d is distance between adjacent lattice planes in the crystal. Moreover, the mean crystallite size was calculated using the Scherrer equation [28]:

$$D = k\lambda/\beta\cos\theta$$

Where λ is the wavelength of X-ray radiation, K is usually 0.89 is the Scherrer constant, λ = 1.54056 Å is the wavelength of the X-ray radiation, β is the peak full width at half maximum in radians and θ is the Bragg diffraction angle. The estimated values of grain size are in 30-40 nm range. The results are summarizes in Table 1.

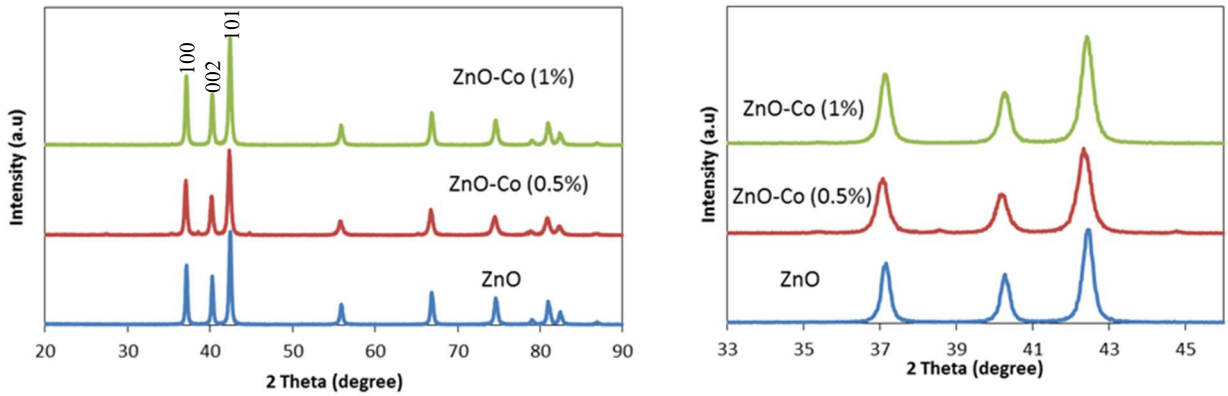


**Fig. 4.** (a) XRD spectrum of undoped ZnO and Co-doped ZnO, (b) Peak position shifting.

**Table 1.** Peak position, band gap, lattice constants and mean crystal size of undoped and Co-doped ZnO.

| Samples | (101) Peak position (degree) | a (100) (Å) | c (002) (Å) | Mean crystal size (nm) | Wavelength (nm) | Band gap (eV) |
|---|---|---|---|---|---|---|
| ZnO | 42.4716 | 3.2547 | 5.6373 | 36.63 | 354 | 2.82 |
| CO-ZnO (0.5%) | 42.2949 | 3.2538 | 5.6352 | 33.57 | 365 | 2.65 |
| CO-ZnO (1.0%) | 42.4282 | 3.2508 | 5.6316 | 33.59 | 381 | 2.52 |

Table 1 also, shows that calculated lattice parameters of the samples. Lattice parameters of Co–ZnO were slightly less than those of ZnO, confirming that the Co ions doped into the ZnO crystal lattice without changing the wurtzite structure. On the other hand, Zinc and cobalt have ionic radius of 0.60 Å and 0.58 Å, respectively. Hence, if Co replaces Zn in the ZnO crystal lattice, a reduction in lattice parameters is expected. As shown in table 1, the c-axis lattice parameter decreased from 5.6373 Å to 5.6352 and 5.6316 Å as the dopant level increased from 0% to 0.5 and at 1% respectively, indicative of Co-atoms replacing zinc atoms in the ZnO lattice [29,30].

### *3.4. SEM and EDAX analysis*

Fig. 5. displays the SEM images of the synthesized undoped and Co-doped ZnO with different molar ratio of dopant. This image reveals that the samples have size of 15-50 nm. The energy Dispersive X-ray spectroscopy (EDAX) analysis (Fig. 6) manifests that the sample are composed of Zn, Co and O.

### *3.5. Photocatalytic activity of the samples*

To evaluate the photocatalytic activity of the synthesized samples, the solution of methylene blue (with a concentration of 5 ppm) in deionized water was selected as a pollutant solution for photodegradation.

The change in concentration of MB for different time intervals is shown in Fig. 7. The result shows that, compared with the undoped ZnO, Co-ZnO nanostructures obviously display a higher photo-catalytic activity.

It is well-known that, the semiconductor photocatalysis is based on the generation of electron ($e^-$) –hole (h+) pair upon UV light irradiation. The electron can be migrated from the valence band to the conduction band, leaving behind hole in the valence band [31].

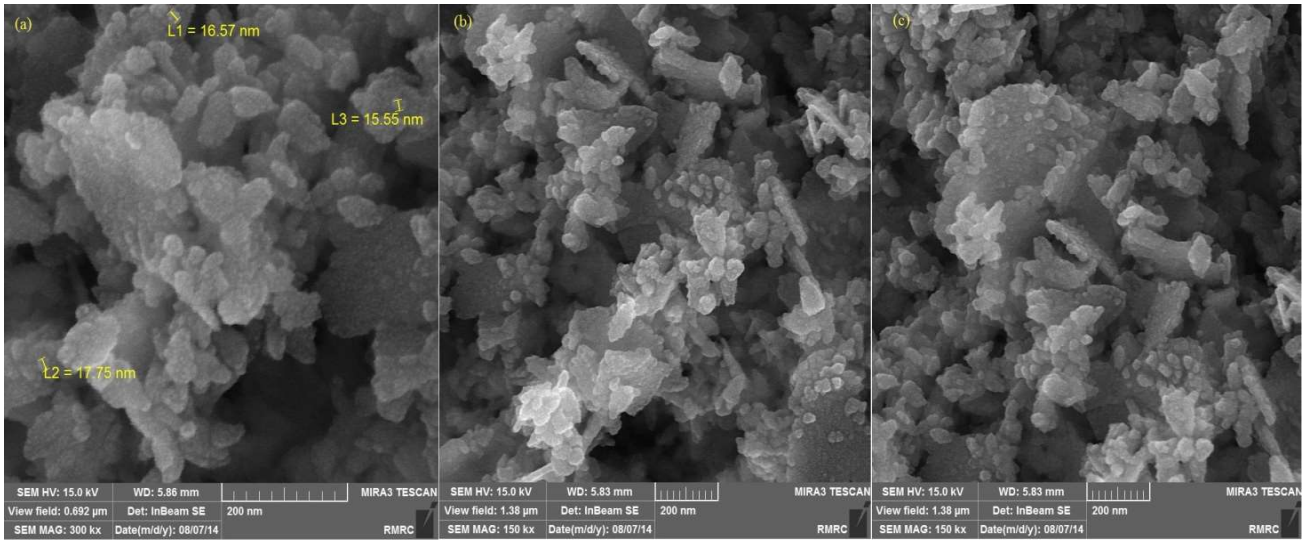


**Fig. 5.** FE-SEM images of (a) undoped ZnO (b) Co-doped ZnO (0.5%) and (c) Co-doped ZnO (1%).

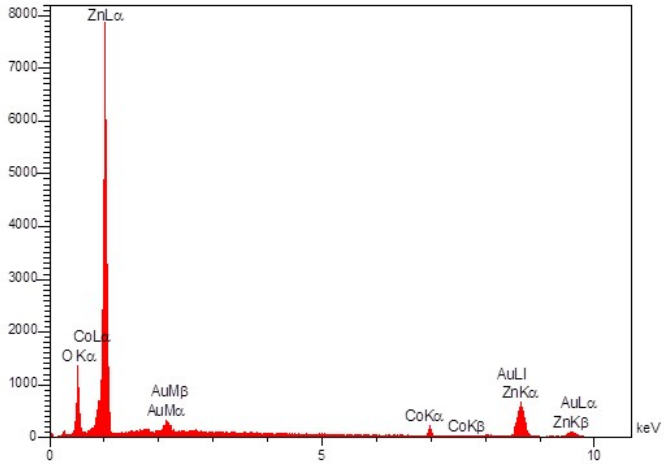


**Fig. 6.** EDAX analysis of Co-doped ZnO (1%).

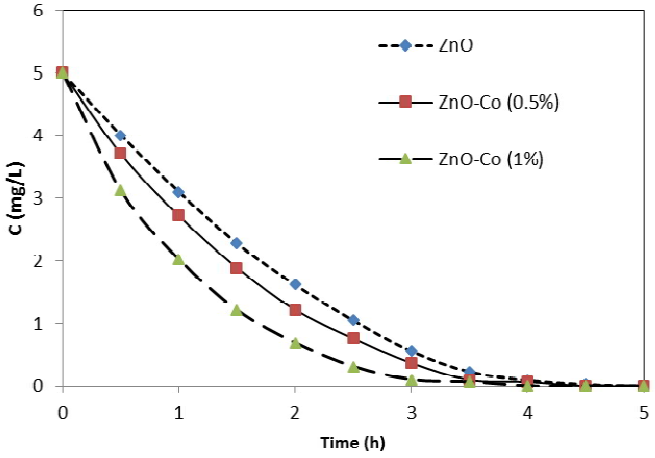


**Fig. 7.** Photodegradation of methylene blue (MB) using the samples.

If the charge separation is maintained, the electron and hole could migrate to the semiconductor surfaces where they participate in redox reactions with the adsorbed organic species [32,33].

Based on the above results, the Co-ZnO nanostructure exhibited more effective electron–hole separation under UV–Vis light irradiation since these substitutions in ZnO lattice could act as the trapping for electron and hole [34]. Hence, the surface redox process by photo generated electrons and holes occur more easily, and the photocatalytic activity of ZnO has significantly improved correspondingly [35].

## 4. Conclusions

Zinc oxide nanoparticles doped with Cobalt have been synthesized by a sonochemical method and have been used as a catalyst in the process of photo degradation of methylene blue as a dye model. According to results, the red shift in band edge absorption peak in UV-Vis absorbance spectrum with increasing metal content has observed and has verified the doping of metal in ZnO nanostructure. Moreover, the band gap of samples was analyzed by Tauc's approach and calculations confirmed that application of cobalt ion as a dopant and dopant concentration are very effective on band gap of ZnO. Based on the experimental results obtained in this study, the existence of cobalt in ZnO structure enhanced the photo degradation efficiency.

## Acknowledgements

We gratefully acknowledge the University of Qom and the Payam Noor University for the support of this work.

## References

[1] P. Mishra, R.S. Yadav, A.C. Pandey, Ultrason. Sonochem. 17 (2010) 560–565.
[2] Y. Yoshino, T. Makino, Y. Katayama, T. Hata, Vacuum 59 (2000) 538–545.
[3] M.H. Habibi, E. Askari, Iran. J. Catal. 1 (2011) 41–44.
[4] H. R. Pouretedal, M. Ahmadi, Iran J. Catal. 3 (2013) 149–155.
[5] M. Fu, Y. Li, S. wu, P. Lu, J. Liu, F. Dong, Appl. Surf. Sci. 258 (2011) 1587–1592.
[6] P. Jongnavakit, P. Amornpitoksuka, S. Suwanboon, N. Ndiege, App. Surf. Sci. 258 (2012) 8192–8198.
[7] B. Wang, J. Iqbal, X. Shan, G. Huang, H. Fu, R. Yu, D. Yu, Mater. Chem. Phys. 113 (2009) 103–106.
[8] R.S. Yadav, P. Mishra, A.C. Pandey, Ultrason. Sonochem. 15 (2008) 863–868.
[9] L. Vayssieres, Adv. Mater. 15 (2003) 464–466.
[10] L. Vayssieres, K. Keis, S. E. Lindquist, A. Hagfeldt, J. Phys. Chem. B 105 (2001) 3350–33502.
[11] L. Vayssieres, K. Keis, A. Hagfeldt, S. E. Linquist, Chem. Mater. 13 (2001) 4395– 4398.
[12] L.E. Greene, M. Law, J. Goldberger, F. Kim, J.C. Johnson, Y. Zhang, R.J. Saykally, P. Yang, Angew. Chem. Int. Edn. Engl. 42 (2003) 3031–3034.
[13] B. Lin, H.C. Zeng, J. Am. Chem. Soc. 125 (2003) 4430-4431.
[14] M. Samadi, H. Asghari Shivaee., M. Zanetti, A. Pourjavadic, A. Moshfegha J. Mol. Catal. A: Chem. 359 (2012) 42– 48.
[15] Y. Ni, X. Wei, J. Hong, Y. Ye, Mater. Sci. Eng. B 121 (2005) 42– 47.
[16] M. Bordbar, B. Khodadadi, N. Mollatayefe, A.Yeganeh- Faal, J. App. Chem. 8 (2013) 43– 47.
[17] M. Srivastava, A.K. Ojha, S. Chaubey, P.K. Sharma, A.C. Pandey, J. Alloy. Compd. 494 (2010) 275–284.
[18] A. Al-Hajry, A. Umar, Y.B. Hahn, D.H. Kim, Superlattice Microst. 45 (2009) 529–534.
[19] H. Fu, C. Pan, W. Yao, Y. Zhu, J. Phys. Chem. B 109 (2005) 22432–22439.
[20] R.A. Nyquist, C.L. Putzig, R.O. Kagel, M.A. Leugers, Academic press, 1971.
[21] R. Mohana, K. Krishnamoorthy S. Kima, Solid State Commun. 152 (2012) 375–380.
[22] J.C. Sin, S.M. Lam, K.T. Lee, A.R. Mohamed, Mater. Lett. 91 (2013) 1–4.
[23] X. Zhou, Y. Li, T. Peng, W. Xie, X. Zhao, Mater. Lett. 63 (2009) 1747–1749.
[24] S. Anandana, N. Ohashib, M. Miyauchi, Appl. Catal. B: Environ. 100 (2010) 502–509.
[25] B. Donkova, D. Dimitrov, M. Kostadinov, E. Mitkova, D. Mehandjiev, Mater. Chem. Phys. 123 (2010) 563-568.
[26] C. Wu, L. Shen, H. Yu, Y.C. Zhang, Q. Huang, Mater. Lett. 74 (2012) 236–238,
[27] J. Zhong, J. Li, X. He, J. Zeng, Y. Lu, W. Hu, K. Lin, Curr. Appl. Phys. 12 (2012) 998–1001.
[28] A. Patterson, Phys. Rev. 56 (1939) 978-982.
[29] X.C. Liu, E.W. Shi, Z.Z. Chen, H.W. Zhang, B. Xiao, L.X. Song, Appl. Phys. Lett. 88 (2006) 252501–252503.
[30] R. Hea, R. K. Hockingb, T. Tsuzukia, Mater. Chem. Phys. 132 (2012) 1035-1040.
[31] Y.H. Zheng, C.Q. Chen, Y.Y. Zhan, X.Y. Lin, Q. Zheng, K.M. Wei, J.F. Zhu, Y.J. Zhu, Inorg. Chem. 46 (2007) 6675-6682.
[32] N. Daneshvar, D. Salari, A.R. Khataee, J. Photochem. Photobiol. A: Chem. 162 (2004) 317-322.
[33] X. Qiu, G. Li, X. Sun, L. Li, X. Fu, Nanotechnology 19 (2008) 215703-21711.
[34] K.C. Barick, S. Singh, M. Aslam, D. Bahadur, Microporous Mesoporous Mater. 134 (2010) 195–202.
[35] L.Wang, Q. Hu., Z. Li, J. Guo, Y. Li, Mater. Lett. 79 (2012) 277–280.